STABILITY OF GAS CLOUDS IN GALACTIC NUCLEI: AN EXTENDED VIRIAL THEOREM

Xian Chen[1], Pau Amaro-Seoane[2] & Jorge Cuadra[1]
Draft version June 30, 2015

ABSTRACT

Cold gas entering the central 1 to 10^2 pc of a galaxy fragments and condenses into clouds. The stability of the clouds determines whether they will be turned into stars or can be delivered to the central supermassive black hole (SMBH) to turn on an active galactic nucleus (AGN). The conventional criteria to assess the stability of these clouds, such as the Jeans criterion and Roche (or tidal) limit, are insufficient here, because they assume the dominance of self-gravity in binding a cloud, and neglect external agents, such as pressure and tidal forces, which are common in galactic nuclei. We formulate a new scheme for judging this stability. We first revisit the conventional Virial theorem, taking into account an external pressure, to identify the correct range of masses that lead to stable clouds. We then extend the theorem to include an external tidal field, crucial for the stability in the region of interest – in dense star clusters, around SMBHs. We apply our *extended Virial theorem* to find the correct solutions to practical problems that until now were controversial, namely, the stability of the gas clumps in AGN tori, the circum-nuclear disk in the Galactic Center, and the central molecular zone of the Milky Way. The masses we derive for these structures are orders of magnitude smaller than the commonly-used Virial masses (equivalent to the Jeans mass). Moreover, we prove that these clumps are stable, contrary to what one would naively deduce from the Roche (tidal) limit.

Subject headings: hydrodynamics – instabilities – ISM: kinematics and dynamics – galaxies: active – galaxies: nuclei

1. INTRODUCTION

An essential ingredient in galaxy formation and evolution is the impact of the growth of supermassive black holes (SMBHs) on the galactic environment (Kormendy & Ho 2013). The agent is gas – a small amount of cool gas with low angular momentum fuels the central SMBH, turning on an active galactic nucleus (AGN), which by means of radiation and outflow heats the gas content on larger, galactic scales, hence regulating the star formation rate in the entire galaxy and possibly cutting off the gas supply to the AGN (McNamara & Nulsen 2007; Fabian 2012).

A bottleneck occurs when cold gas is funneled to the nuclear region of a galaxy and forms a disk (because of angular-momentum conservation), at a distance of a few hundreds to several parsec (pc) from the SMBH. At this stage, the gas density rises to the critical point of triggering the Jeans instability, and hence the gaseous disk fragments and becomes clumpy (Shlosman et al. 1990; Goodman 2003). From this point on, the inflow of gas is carried on mainly by clouds. But it is known that a cloud produced by the Jeans instability is self-gravitating, and will collapse on the free-fall timescale. The consequence is that within a short time most clouds would turn into stars, so essentially, and contradictory to many observations, little gas is left to fuel the central AGN (Goodman & Tan 2004; Tan & Blackman 2005; Collin & Zahn 2008).

To resolve this contradiction, several ideas have been proposed. In particular, two possibilities to deliver gas

clouds to the AGN in spite of them being Jeans unstable have been considered. (i) A cloud can be stabilized by a strong magnetic field or fast rotation (Rees 1987; Vollmer & Duschl 2001b). (ii) The inflow of gas could be accelerated, as a result of an asymmetric gravitational potential (Shlosman et al. 1990; Maciejewski et al. 2002) or cloud-cloud collisions (Krolik & Begelman 1988; Kumar 1999; Vollmer et al. 2004), so that gas clouds can be delivered to the vicinity of SMBHs before turning into stars.

An alternative viewpoint is that the gas clouds, after the initial fragmentation, have gone through a series of physical changes, so that the eventual physical properties no longer satisfy the Jeans criterion. Two physical processes could cause such changes: (i) Big clouds could break into smaller ones due to rapid cooling (Burkert & Lin 2000). Each descendant cloud can be stable because of the reduced self-gravity. A galactic nucleus is an ideal place of producing such clouds, because the high gas density there enhances the cooling rate. (ii) Collisions between gas clouds are frequent in galactic nuclei, since the number density of cloud is high and the orbital periods are short (Krolik & Begelman 1988). Such collisions raise the internal pressure of a cloud, supporting it against gravitational collapse.

It is possible today to test the stability of gas clouds with observational data. (i) Clumps have been seen in the central hundreds of pc of many galaxies, quiescent and active (Hunt & Malkan 2004; Mazzalay et al. 2013; Davies et al. 2014). (ii) For AGNs, it has been widely accepted that a clumpy, dusty torus with a size of several pc must exist surrounding the SMBH to cause the type I/type II dichotomy (Krolik & Begelman 1988; Antonucci 1993). Indeed, direct evidence of such clumps has been found by modeling the X-ray variability of AGNs,

[1] Instituto de Astrofísica, Facultad de Física, Pontificia Universidad Católica de Chile, 782-0436 Santiago, Chile; E-mail: xchen@astro.puc.cl
[2] Max Planck Institut für Gravitationsphysik (Albert-Einstein-Institut), D-14476 Potsdam, Germany; E-mail: Pau.Amaro-Seoane@aei.mpg.de

so that we have a way of measuring some of the clouds' physical properties (Risaliti et al. 2002; Markowitz et al. 2014,and references therein). (iii) In the Milky Way, about 200 molecular clumps have been found (Miyazaki & Tsuboi 2000; Oka et al. 2001) within a distance of 200 pc from the Galactic Center (GC), in the region known as the "central molecular zone" (CMZ, Mezger et al. 1996). Further inside, at a distance of 1 to 3 pc from Sgr A* (the SMBH, 8 kpc from Earth), there is the circum-nuclear disk (CND), which has been resolved into about 30 molecular clumps whose orbits are mostly circular (Genzel et al. 1985; Jackson et al. 1993; Marr et al. 1993; Marshall et al. 1995).

To analyze the stability of the observed clumps, a criterion is required. However, the conventional Jeans criterion and Roche limit become insufficient, because they regard self-gravity as the only force binding a gas cloud, which is not true in galactic nuclei. Here gas clouds are likely subject to a compression by a high external pressure. This pressure exists because the interstellar medium (ISM) in the nuclear region of a galaxy usually has a high density and a large turbulent velocity. Moreover, there is likely a strong tidal force acting onto the clouds, because of the ubiquity of SMBHs and dense nuclear star clusters (see Amaro-Seoane 2012, for a review). Here we show that these agents are crucial in determining whether a cloud is stable, as well as in the correct derivation of its mass.

The paper is organized as follows. In Section 2, we revisit the Virial theorem so as to link the physical properties of a gas cloud to its environmental conditions, including the external pressure (Section 2.1) and the background tidal field (Section 2.2). After taking these external factors into account, we formulate in Section 2.3 our "*extended Virial theorem*", which gives only one stable solution for the mass, and we discuss its implications. In the light of this stable solution, we proceed in Section 3 to interpret the observational data of gas clumps, including those in AGN tori (Section 3.1), the CND (Section 3.2), and the CMZ (Section 3.3) of the Milky Way. Finally in Section 4, we justify the assumptions that we adopted in the work, and we discuss the implications of the results.

2. VIRIAL THEOREM

2.1. *External Pressure*

A strong external pressure affects the motion of the fluid at the surface of a gas cloud, and changes the condition of stability of the entire cloud. Such a high pressure is found in galactic nuclei because of a concentration of hot ionized- and turbulent cold gas. The Virial theorem (Clausius 1870) accounting for an external pressure has been derived in the past (Spitzer 1978; Shu 1992) and has been applied to the molecular clouds in the CMZ of the Milky Way (e.g. Miyazaki & Tsuboi 2000; Oka et al. 2001). In this subsection we present the derivation in detail so as to highlight an important list of conceptual points – which are often overlooked in the literature – that will be crucial for the main ideas of this work.

Without magnetic fields and tidal forces affecting it, the equation of motion of a fluid element can be written as:

$$\rho \ddot{\mathbf{r}} = -\nabla P - \rho \nabla \Phi_c, \qquad (1)$$

where ρ is the fluid density, $\mathbf{r}$ is its position vector, the dots denote time derivatives, P is the internal pressure including both thermal and turbulent motion, and Φ_c is the gravitational potential (self-gravity). If we take dot product with $\mathbf{r}$ on both sides of the last equation and integrate it over the entire volume of the cloud, the left-hand-side (LHS) of Equation (1) becomes

$$\int_V \rho \left(\mathbf{r} \cdot \ddot{\mathbf{r}} \right) dV = \frac{1}{2} \frac{D^2}{Dt^2} \int_V \rho r^2 dV - \int_V v^2 \rho dV. \qquad (2)$$

If the internal structure of the cloud is steady, the first term on the right-hand-side (RHS) of Equation (2) vanishes because ρr^2 is constant. If the cloud is also not rotating, the second term vanishes, because v, the macroscopic velocity of a fluid element, is zero.

Since we are integrating Equation (1), when the integral of the LHS is zero, the integrated RHS must also be zero:

$$0 = -\int_V \left(\mathbf{r} \cdot \nabla P + \rho \mathbf{r} \cdot \nabla \Phi_c \right) dV \qquad (3)$$

$$= \int_V \left[P \nabla \cdot \mathbf{r} - \nabla \cdot (\mathbf{r} P) \right] dV - \int_V \left(\mathbf{r} \cdot \nabla \Phi_c \right) dm \qquad (4)$$

$$= \int_V 3P dV - \int_S P_S \mathbf{r} \cdot d\mathbf{S} + \int_V \mathbf{r} \cdot \mathbf{a}_{gr} dm, \qquad (5)$$

where P_S denotes the pressure at the surface of the cloud, $dm = \rho \, dV$ is the mass of the fluid element, $d\mathbf{S}$ is the differential area vector orthogonal to the surface of the cloud, and we have introduced for convenience $\mathbf{a}_{gr} \equiv -\nabla \Phi_c$, the self-gravity of the cloud. We now assume spherical symmetry and homogeneity for the cloud to simplify the integration. We note however that this assumption does not have an impact in the general conclusions that we will draw. Homogeneity leads to a constant density ρ and a constant one-dimensional velocity dispersion σ inside the cloud, so $P = \rho \sigma^2$ is also constant. In addition with the assumption of sphericity, Equation (5) reduces to

$$4\pi R_c^3 P_S = 3M\sigma^2 - aGM^2/R_c, \qquad (6)$$

the conventional Virial theorem for a steady, non-rotating cloud embedded in a pressurized medium. Here R_c is the radius of the cloud, M is the cloud mass, G is the gravitational constant, and a is a geometrical factor of order unity, which is $3/5$ assuming sphericity.

The connection between the above Virial theorem and the external pressure P_{ext} comes through the surface pressure P_S – a cloud in hydrostatic equilibrium with the surrounding medium will have $P_S = P_{ext}$. When $P_{ext} = 0$, Equation (6) has only one non-trivial solution $M_0 := M = 3R\sigma^2/(aG)$, that is *the commonly-used virial mass* in the literature (e.g., Zwicky 1937). It can be easily verified that M_0 is essentially the same as the Jeans mass $M_J = \lambda_J^3 \rho$ (differ by only a factor of 1.02), where $\lambda_J = \sigma \sqrt{\pi/(G\rho)}$ is the Jeans length.

In a more general situation, which is what defines the fundamentals of this research, $P_{ext} > 0$, and then two non-trivial solutions exist for M in Equation (6), as is illustrated in Figure 1. The two solutions $M_{\pm}$ (and we
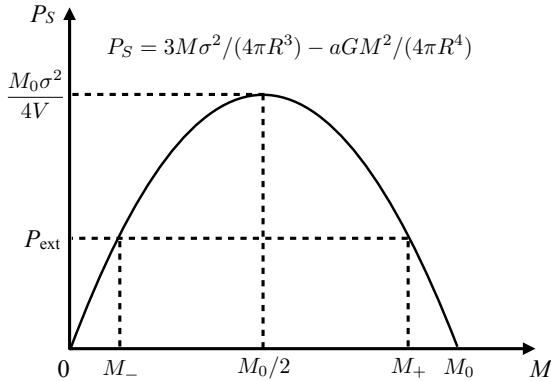
FIG. 1.— Surface pressure P_S as a function of mass M for a spherical, virialized cloud with constant radius R_c and internal velocity dispersion σ. Given an arbitrary external pressure P_{ext} between 0 and the characteristic pressure $M_0\sigma^2/(4V)$, two solutions exist for M that allow the cloud to be in hydrostatic equilibrium, i.e. $P_S = P_{\text{exp}}$. One solution, M_+, which is unstable (see text), falls in the mass range between the commonly used virial mass, $M_0 = 3R\sigma^2/(aG)$, and half of it, $M_0/2$. The other solution, M_-, is stable and has a maximum value of $M_0/2$.

note that we adopt the notation of Oka et al. 2001, with $M_+ \geq M_-$), can be expressed in a compact format

$$M_\pm = \alpha_\pm M_0, \text{ with } \alpha_\pm := \frac{1 \pm \sqrt{1-\beta}}{2}, \qquad (7)$$

where we have defined the dimensionless mass $\alpha := M/M_0$ and the dimensionless surface pressure $\beta := 4P_SV/(M_0\sigma^2)$, where $V = 4\pi R_c^3/3$ is the volume of the cloud.

Thanks to these dimensionless parameters, we can rewrite Equation (6) in a dimensionless way: $\beta = 4\alpha - 4\alpha^2$, which is useful to understand the role of these parameters in assessing the correct values for the mass of the cloud, as we will see later. Figure 2 displays the geometric meaning of these dimensionless parameters.

A close analysis of Equation (6) reveals crucial information about the stability of gas clouds in galactic nuclei:

1. Given (for fixed) R_c and σ – quantities that can be extracted from observations – the maximum P_S that a cloud can have is $M_0\sigma^2/(4V)$. This is also the maximum external pressure that a cloud can withstand in hydrostatic equilibrium. At this critical point (because it is an inflection point, see Figure 1), $P_{\text{ext}} = M_0\sigma^2/(4V)$, the only solution to maintain hydrostatic equilibrium of the cloud is $M = M_0/2$.

2. When $0 < P_{\text{ext}} < M_0\sigma^2/(4V)$, we have that $M_0/2 < M_+ < M_0$ and $0 < M_- < M_0/2$. Hence, in this regime of P_{ext}, M_0 is *always* an overestimation of the *real* mass of the cloud.

3. Only one branch of the solution for the mass of the cloud is *dynamically stable*. To see this, let us consider a cloud already in hydrostatic equilibrium, and then we perturb it by either increasing or decreasing its mass. (i) First branch: $M = M_+$.
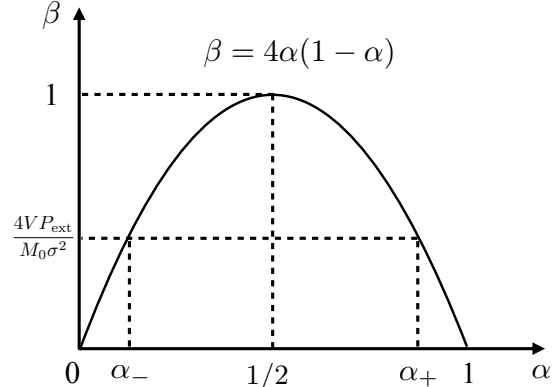

FIG. 2.— Same as Figure 1 but plotting the dimensionless quantities. The mass M of a cloud is normalized by the commonly-used virial mass M_0, so that $\alpha = M/M_0$. The surface pressure P_S is normalized by the characteristic pressure $M_0\sigma^2/(4V)$, so $\beta = 4P_SV/(M_0\sigma^2)$.

If we slightly increase M, the surface gravity of the cloud increases, meanwhile the surface pressure of the cloud decreases because $dP_S/dM < 0$, as shown in Figure 1. The tendency of the cloud is to shrink, but this will increase the surface gravity even more, so the cloud collapses. On the other hand, if we slightly decrease M, then the surface gravity decreases while P_S increases, so the cloud will expand, which leads to an even smaller surface gravity, therefore the cloud eventually explodes. (ii) However, for the second branch of the solution, $M = M_-$, we have $dP_S/dM > 0$, so the cloud is in the opposite situation – P_S changes in proportion with the change of the surface gravity. Now the cloud is dynamically stable.

4. As a consequence of the last point, we can see that only M_- is physically correct. Observationally, gas clouds are often found in places where the observed pressure (i.e. not derived from the Virial theorem) is such that $P_{\text{ext}} \ll M_0\sigma^2/(4V)$, or $\beta \ll 1$ in the dimensionless expression, as we will see later in the practical examples. Hence, a common practice in the literature is to use $P_S = 0$ as an approximation (without any justification a priori). As a result, the only non-trivial solution of Equation (6) is $M = M_0$, which is the commonly-used virial mass. Nonetheless, we know that there are, strictly speaking, two solutions for M even when P_S is very small, and that M_0 is an approximation to the M_+ solution. This M_0 *cannot* be the real mass of the cloud because (i) it is, at best, its upper limit, (ii) it is on the *unstable* branch for the solution of M, and (iii) connected to the first reason, it can overestimate the cloud mass (mostly likely M_-) by orders of magnitude, since $M_0/M_- = 1/\alpha_- \gg 1$ when $\beta \ll 1$.

Point (4) highlights the necessity of including external forces in the analysis of the stability of clouds, no matter how small the external forces may be. This point is often overlooked in the literature. The root of this ignorance

is the intuition that self-gravity is the dominant binding force in clouds.

This intuition is fallacious, as one can see by evaluating the relative importance of the two binding forces in the Virial theorem, i.e. comparing the external pressure term $4\pi R_c^3 P_S$ and the self-gravity term aGM^2/R_c in Equation (6). Their ratio, $(1-\alpha)/\alpha$, is greater than 1 for a dynamically stable cloud, i.e. external pressure predominates, because we have proven that α must be smaller than $1/2$ to qualify as a stable solution. If the ratio is smaller than 1, i.e. if the self-gravity predominates, the value of α cannot be elsewhere but greater than $1/2$, and we have proven that such a solution is dynamically unstable.

2.2. *Tidal Terms*

A galactic nucleus, which is the focus of this work, usually has a SMBH sitting at the centre with a dense (nuclear) star cluster surrounding it. Their presence introduces in our problem an additional ingredient of tidal fields, which will result in new terms to be added to the Virial theorem.

Besides feeling tidal forces, our test cloud is very likely to have a certain degree of rotation as well. This is so because its orbital motion in the galactic nucleus leads to periodic tidal perturbations, which in the long run tends to synchronize the spin of the cloud with its orbital period (Gladman et al. 1996). At this point, we say that the cloud is "tidally locked". In this subsection, we will include the effects of rotation in our analysis by exploring two representative cases: (i) When the cloud is non-rotating with respect to the rest frame – the observer on the Earth – and (ii) when it is already tidally locked.

In the following, we will show that (a) the Virial theorem without tidal forces, (b) the Virial theorem with tidal forces but no rotation, and (c) the Virial theorem with tidal forces and a tidally-locked cloud can all be merged into a new, universal theorem.

We start our analysis by adding in Equation (1) an external gravitational potential Φ_{ext}, accounting for both the SMBH and the nuclear star cluster. The equation of motion of a fluid element inside our test cloud hence becomes

$$\rho\ddot{\mathbf{R}} = -\nabla P - \rho\nabla\Phi_c - \rho\nabla\Phi_{\text{ext}}. \qquad (8)$$

In the last equation we have introduced $\mathbf{R}$ as a position vector for the fluid element with its origin at the SMBH, which we assume to be at the galactic centre. We now introduce a new position vector, $\mathbf{D}$, which has the same origin but points at the Centre-of-Mass (CoM) of the cloud. The difference of the two, $\mathbf{R} - \mathbf{D}$, is a vector that points from the CoM to the fluid element of the cloud, which we name $\mathbf{r}$. Figure 3 illustrates the definitions of the vectors. These new vectors allow us to re-write the last equation as follows:

$$\rho\ddot{\mathbf{r}} = -\nabla P - \rho\nabla\Phi_c + \underbrace{\rho[-\nabla\Phi_{\text{ext}}(\mathbf{R}) - \ddot{\mathbf{D}}]}_{\text{tidal term, }\rho\,\mathbf{a}_t}. \qquad (9)$$

In the brackets we can now easily identify – thanks to the introduction of $\mathbf{D}$ and $\mathbf{R}$ – the tidal acceleration $\mathbf{a}_t$.
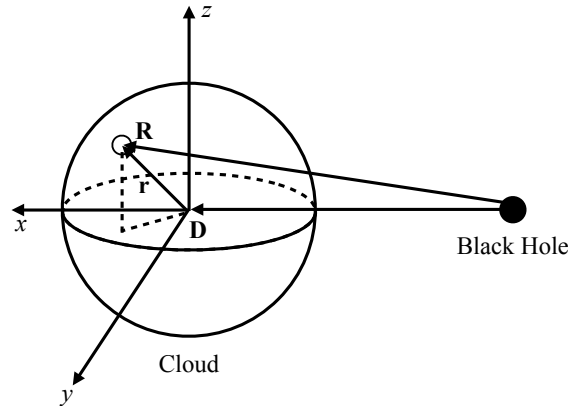

FIG. 3.— Reference frame for a fluid element inside a non-rotating cloud which is orbiting a SMBH. Starting from the SMBH, the vector $\mathbf{R}$ points to the fluid element and $\mathbf{D}$ points to the CoM of the cloud. The coordinates are chosen in a way such that the origin coincides with the CoM of the cloud, the x-axis points in the same direction as $\mathbf{D}$, and the z-axis is perpendicular to the orbital plane of the cloud. In this coordinate system, the vector $\mathbf{R} - \mathbf{D}$ is pointing from the CoM of the cloud to the fluid element, which we denote as $\mathbf{r}$, and its three components are (x, y, z).

We now proceed the same way as we did in Section 2.1 – take the dot product with respect to $\mathbf{r}$ and integrate Equation (9) over the volume of the cloud. The integration is different depending on whether the cloud is rotating or not.

2.2.1. *Non-rotating Clouds*

In this case, the orientation of $\mathbf{r}$ is fixed with respect to an observer standing on the earth, so that the integration is almost straightforward. As a matter of fact, the integration has already been done in Section 2.1 (see Equations 2 to 6) except for the last tidal term $\rho\,\mathbf{a}_t$.

To complete the integration, we need to know the three components of the vector $\mathbf{a}_t$, so we have to define our working coordinates. As is illustrated in Figure 3, we choose the origin of coordinates at the CoM of the cloud. The x-axis is chosen to be aligned with $\mathbf{D}$ and the z-axis aligned with the *orbital* angular momentum of the cloud. Hence, $\mathbf{r} = (x, y, z)$. We define ω_c to be the angular velocity of a circular orbit at a distance of D from the SMBH, so that $\ddot{\mathbf{D}} = (-\omega_c^2 D, 0, 0)$ if the nuclear star cluster is spherically symmetric.

Given that $|\mathbf{r}| \ll |\mathbf{D}|$ in the system of our interest, we do a linear expansion for the components of $\mathbf{a}_t$ and find

$$\mathbf{a}_t = (xT, -y\omega_c^2, -z\omega_c^2). \qquad (10)$$

Here we have introduced $T = -Dd\omega_c^2/dD$, the tidal acceleration per unit length in the radial direction (e.g. Stark & Blitz 1978). The two components with negative signs correspond to compressive tides: A fluid element moving away from the CoM of the cloud will experience a restoring acceleration in the y and z directions. Given that T is positive in galaxies (as we will see later), the acceleration in the x direction is pointing away from the CoM.

Therefore, we have seen that the tidal forces acting on the cloud is not spherically symmetric. Consequently, a
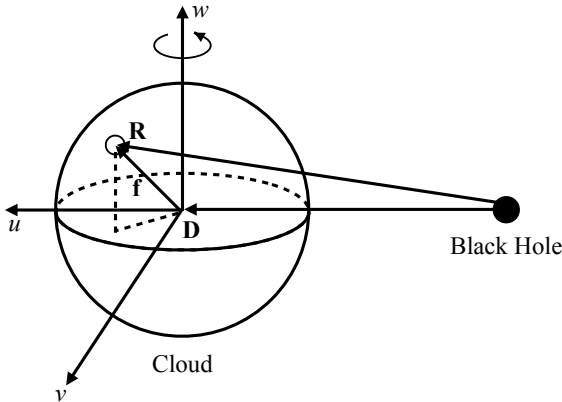
FIG. 4.— Reference frame for a fluid element in a rotating cloud. The two position vectors, $\mathbf{R}$ and $\mathbf{D}$, and the origin of the coordinates are defined in the same way as in Figure 3, but the orientations of the coordinates are not. Here, the w-axis is defined by the rotating axis of the cloud, and the other two orthogonal axes, namely u- and v-axes, are co-rotating with the cloud. Now we denote the vector $\mathbf{R} - \mathbf{D}$ as $\mathbf{f}$, to distinguish it from the $\mathbf{r}$ vector in the non-rotating case, and in the current coordinate system $\mathbf{f}$ has three components (u, v, w). If the cloud is tidally locked, the w-axis will be perpendicular to the orbital plane of the cloud.

cloud in hydrostatic equilibrium is not strictly spherical. However, for mathematical simplicity, we inherit sphericity for the later analysis and we deem this approximation valid to first-order. This small sacrifice of mathematical accuracy will reward us with useful physical insights, as we will see. Now using the three components of $\mathbf{a}_t$ and assuming sphericity, we derive

$$\int_V \mathbf{r} \cdot \mathbf{a}_t dm = bR^2 M(T - 2\omega_c^2),\qquad(11)$$

where $b = 1/5$ for spherical, homogeneous clouds.

2.2.2. *Rotating, Tidally-locked Clouds*

The second representative case in our study is a cloud that is tidally locked in its orbit around the SMBH. In this case, the integral of the LHS of Equation (9), i.e. Equation (2), is no longer zero. To address the calculation, we now choose a more convenient frame, the one centered on the CoM of the cloud and co-rotating with it. Figure 4 illustrates this co-rotating frame.

From the CoM to a fluid element in the cloud, the position vector is defined to be $\mathbf{f} := u\,\mathbf{e}_u + v\,\mathbf{e}_v + w\,\mathbf{e}_w$, with $\mathbf{e}_i$ ($i \equiv u, v, w$) the unity vector of components. As in the previous non-rotating case, the relation $\mathbf{R} = \mathbf{D} + \mathbf{f}$ still holds. Therefore, starting from Equation (8), we derive the equation of motion for the considered fluid element as:

$$\rho\ddot{\mathbf{f}} = -\nabla P - \rho\nabla\Phi_c + \rho\,\mathbf{a}_t.\qquad(12)$$

This equation is similar to Equation (9), except that the unit vectors that we choose for $\mathbf{f}$ are rotating respect to an observer on Earth. As a result of this choice, $\ddot{\mathbf{f}}$ is a combination of two accelerations, i.e.

$$\ddot{\mathbf{f}} = \underbrace{(\ddot{u},\,\ddot{v},\,\ddot{w})}_{\text{In the rotating frame}} - \underbrace{\mathbf{a}_{\text{cen}}}_{\text{centrifugal}},\qquad(13)$$

where the acceleration $\mathbf{a}_{\text{cen}}$ comes from the usual concept of a centrifugal force. Let us consider now the consequences for the integration:

- The first acceleration corresponds to the motion of a fluid element with respect to the chosen frame. Because we have chosen the co-rotating frame, the fluid elements of the cloud are "frozen" with respect to the frame, so an integration of the dot product of this acceleration with $\mathbf{f}$ will vanish, exactly as in Equation (2).

- As for the centrifugal acceleration, the integral $\int_V \mathbf{f} \cdot \mathbf{a}_{\text{cen}} dm$ does not vanish because the product $\mathbf{f} \cdot \mathbf{a}_{\text{cen}}$ is always positive, except for those fluids lying on the rotation axis of the cloud, in which case $\mathbf{f} \cdot \mathbf{a}_{\text{cen}}$ will be zero.

After these considerations, we can rearrange Equation (12), moving all the terms with non-vanishing integrals to the RHS, and derive a new, more convenient form for the equation of motion:

$$\rho\,(\ddot{u}, \ddot{v}, \ddot{w}) = -\nabla P - \rho\nabla\Phi_c + \rho\,(\mathbf{a}_t + \mathbf{a}_{\text{cen}}).\qquad(14)$$

We are now left with only one task, namely the integration of the tidal term $\int_V \mathbf{f} \cdot (\mathbf{a}_t + \mathbf{a}_{\text{cen}})\, dm$, because we already know the outcome of the other integrals from the previous subsection.

If the cloud is tidally-locked and on a circular orbit around the SMBH, the angular velocity (or spin) vector $\mathbf{\Omega} = (0, 0, \omega_c)$ will be constant, and the centrifugal acceleration can be calculated with $\mathbf{a}_{\text{cen}} = -\mathbf{\Omega} \times (\mathbf{\Omega} \times \mathbf{f}) = (u\omega_c^2, v\omega_c^2, 0)$. After some algebra we find

$$\int_V \mathbf{f} \cdot (\mathbf{a}_t + \mathbf{a}_{\text{cen}})dm = bR^2 MT,\qquad(15)$$

where, again, we assume sphericity for the cloud.

2.3. *The Extended Virial Theorem*

Before we continue, we recapitulate what we have got so far: (i) The commonly-used virial mass M_0 is inevitably an overestimation of the mass of a dynamically stable cloud. (ii) The tidal forces lead to an extra term in the derivation of the Virial theorem, and we shall call this new theorem the *extended Virial theorem* (EVT hereafter). (iii) We evaluated two representative cases to calculate this extra term, namely a non-rotating cloud, which led to Equation (11), and a tidally-locked cloud, which resulted in Equation (15).

It is easy to see that the EVT takes the form:

$$4\pi R_c^3 P_S = 3M\sigma'^2 - aGM^2/R_c,\qquad(16)$$

if we define σ', the effective velocity dispersion, in the following way:

$$\sigma'^2 = \sigma^2 + bR^2(T - 2\omega_c^2)/3\qquad(17)$$

for non-rotating clouds and

$$\sigma'^2 = \sigma^2 + bR^2 T/3 \qquad (18)$$

for tidally-locked ones. Now it is clear that an external tidal field effectively changes the internal energy of a cloud, in other words, it changes the ability of the cloud to expand or to contract.

The discussion presented in Section 2.1 must be re-evaluated in the light of our newly derived Virial theorem. Here we highlight two crucial points. (i) It can readily be seen that Equation (16) is structurally identical to Equation (6). The only difference is the newly defined σ', which equivalently introduces a new virial mass, $M_0' = 3R\sigma'^2/(aG)$. Correspondingly, the dimensionless mass should be redefined as $\alpha' = M/M_0'$ and the dimensionless surface pressure as $\beta' = 4P_S V/(M_0'\sigma'^2)$, so that the EVT retains a dimensionless form of $\beta' = 4\alpha'(1-\alpha')$. (ii) The ETV is a quadratic function of M, same as the conventional Virial theorem. Therefore, we can prove that given β', the dynamically-stable solution is $M_-' = \alpha_-' M_0'$, where $\alpha_-' < (1/2)$. Again, this solution stands for a cloud bounded mainly by the external forces.

We now rewrite σ' in a different way, so that it is easier to understand what the implications of our EVT are. If the central SMBH has a mass $M_\bullet$ and the nuclear star cluster follows a density profile $\rho_* \propto D^{-\gamma}$ (see Amaro-Seoane 2012, for a review), the angular velocity ω_c of a circular orbit can be written as

$$\omega_c^2 = \frac{G[M_\bullet + M_*(D)]}{D^3}, \qquad (19)$$

where $M_*(D) \propto D^{3-\gamma}$ is the stellar mass enclosed by the orbit. It follows that

$$\sigma'^2 = \sigma^2 + \frac{bR^2}{3}\left[\underbrace{\frac{GM_\bullet}{D^3}}_{\text{black hole}} - \underbrace{(2-\gamma)\frac{GM_*(D)}{D^3}}_{\text{stellar component}}\right] \qquad (20)$$

for the non-rotating clouds

$$\sigma'^2 = \sigma^2 + \frac{bR^2}{3}\left[\frac{3GM_\bullet}{D^3} + \gamma\frac{GM_*(D)}{D^3}\right] \qquad (21)$$

for tidally-locked clouds. It is clear that, as marked in Equation (20), two components contribute to the tidal effects. The first contribution is directly linked to the mass of the SMBH, and the second one to the mass *and shape* of the stellar system.

A close inspection of the last two equations reveals two pieces of new information:

(i) If the cloud is non-rotating, then we could have $\sigma' < \sigma$, i.e. when the SMBH term of Equation (20) becomes smaller than the stellar one. In this case the tidal force is effectively reducing the internal energy of the cloud. This effect is coming from the stellar component, especially its tidal forces in the tangential direction which are acting in a compressive way on to the cloud. On the other hand, we can have the inverse situation, in which $\sigma < \sigma'$, i.e. when the cloud is so close to the SMBH so that the role

of the stellar system can be neglected (very small D). In this latter situation, the tides, induced mainly by the SMBH, essentially are tearing the cloud apart, increasing the internal energy of the cloud.

(ii) In the tidally-locked case, we have a similar situation, because γ is not necessarily always positive (e.g. Merritt 2010). Contrasting the last two equations, one can see that a cloud that is tidally-locked always has a larger σ' than that of a non-rotating one. This excess of effective internal energy comes from the additional centrifugal acceleration.

3. APPLICATIONS

In this section we apply the stable solution from the EVT, i.e. $M_-' = \alpha_-' M_0'$, to infer the physical properties of observed gas clumps in two types of galactic nuclei, namely AGNs and our GC. As we will see, using M_-' instead of the conventional virial mass M_0 resolves a series of controversies and provides interesting implications for the origin and evolution of these clumps.

From now on we will call an observed object a "clump", to distinguish it from the idealized, theoretical concept of a "cloud". This distinction is meaningful because it draws attention to the limitations of the observational data – while clouds have well-defined shapes and physical parameters, clumps do not have clearcut boundaries, nor are all their physical quantities observable.

In each of the three subsections that follow we (i) first introduce the current controversy linked to the usage of the conventional virial mass and (ii) resolve the controversy by applying our EVT.

3.1. *Clumps in AGN Tori*

Controversy: Analysis of the X-ray variability of AGNs indicates the existence of a population of dusty clumps that are very close to the central SMBHs (see Netzer 2015, for a review). The location of these clumps coincides approximately with the inner boundary of the dusty torus (e.g. Elvis 2000; Risaliti et al. 2002). Recent work, such as the one by Markowitz et al. (2014), provides us with the required observable quantities for a clump. We summarize here the typical values for them: (i) A size of $R_c \simeq 2.0 \times 10^{14}$ cm, (ii) a Hydrogen (number) density of about $n_H \simeq 3.5 \times 10^8$ cm^{-3}, (iii) a mass for the central SMBH of $M_\bullet \simeq 4.2 \times 10^7\ M_\odot$, (iv) a distance of $D \simeq 5.0 \times 10^{17}$ cm from the SMBH , and (v) a bolometric luminosity of $L \simeq 1.6 \times 10^{44}$ erg s^{-1} for the AGN. From the size and density, we derive a typical mass of $M = 10^{-5}\ M_\odot$ for a spherical and homogeneous clump.

Naively, one would expect a clump to be tidally dissolved if the tidal force from the SMBH acting on to the clump exceeds its self-gravity. Hence, it would seem that the density of a clumps should be at least

$$n_{\text{tide}} \simeq M_\bullet/(m_p D^3). \qquad (22)$$

From the quoted typical values and a proton mass of $m_p = 1.67 \times 10^{-24}$ g, this critical density is $n_{\text{tide}} \simeq 4.0 \times 10^{11}$ cm^{-3}, a thousand times above n_H. And yet the clumps exist. This paradox led Markowitz et al. (2014) to discuss possible stabilizing mechanisms, including magnetic field and external pressure.

Solution: The aforementioned clump – whose self-gravity is weaker than the external tidal forces but remains bound and stable – is exactly the type of cloud we have found as the stable solution of our EVT (Section 2.3). Our EVT predicts that the clump has a non-negligible surface pressure P_S, and its mass is $\alpha'_- M'_0$ where $\alpha'_- < (1/2)$. Therefore, we equate $\alpha'_- M'_0$ to $10^{-5} M_\odot$, the typical mass of the clump, and we proceed to calculate α'_- and then P_S.

To do so, we have all the data we need except those of σ, γ, and $M_*(D)$. However, it is relatively straightforward to obtain a well-established value for σ. Krolik & Lepp (1989) proved that the typical gas temperature in a molecular cloud in an AGN torus is about 10^3 K. This corresponds to a typical internal velocity of $\sigma \approx 3$ km s^{-1}.

As for γ and $M_*(D)$, which determine the value of σ', we notice that $M_*(D) \ll M_\bullet$ at the distance $D \simeq 0.2$ pc where the clumps are observed. Therefore, we can neglect the stellar components, i.e. those determined by $M_*(D)$ and γ, in the analysis of the tidal terms.

Although the SMBH term predominates in the brackets of Equations (20) and (21), the two terms in the brackets are multiplied by R_c^2. This multiplication leads to a negligibly small contribution compared to σ^2, so essentially $\sigma' \approx \sigma \approx 3$ km s^{-1}. It is important to know in advance that (i) the tidal term from the SMBH is not always negligible, as we will see in Section 3.2, and (ii) neither is the stellar component always negligible, as is shown in Section 3.3.

We have specified the values of all the terms entering the EVT, so we can solve α'_- and P_S. From σ' and R_c we derive $M'_0 \simeq 0.67 M_\odot$. It follows that $\alpha'_- = M/M'_0 \simeq 1.5 \times 10^{-5}$. Since the value we have just derived for α'_- is smaller than $1/2$, the mass $M = 10^{-5} M_\odot$ qualifies as a stable solution in the context of Equation (16). Since we know that α'_- must satisfy the relationship $\beta' = 4\alpha'_-(1-\alpha'_-)$, we derive that $\beta' \simeq 4\alpha'_- \simeq 6.0 \times 10^{-5}$, and from the definition of β' (Section 2.3), we finally find $P_S \simeq 5.4 \times 10^{-5}$ erg cm^{-3}.

Now that we have the value for the surface pressure of a stable *cloud* in our theory, we calculate with observed data the typical external pressure of the environment where real clumps are found and compare the two.

The main source of external pressure is the *turbulent* gas surrounding the clump. Estimating its magnitude requires knowledge of the mean density $n_{\rm ext}$ and the turbulent velocity $v_{\rm ext}$ of such external gas medium. To estimate $v_{\rm ext}$, we recall the following two facts. (i) AGN tori are dusty (Netzer 2015) and dust grains will be destroyed if the collisional velocity induced by turbulence exceeds 120 km s^{-1} (Shull 1978). (ii) The turbulent velocity must also be comparable to the Keplerian velocity, about 10^2 to 10^3 km s^{-1} depending on $M_\bullet$ and D, to maintain the empirically required geometric thickness of the torus (Krolik & Begelman 1988). Taking both facts into account, we adopt $v_{\rm ext} = 100$ km s^{-1}.

For $n_{\rm ext}$, we know that the integrated Hydrogen column density in the mid-plane of the torus is an observable, and the typical value is $N_H \sim 10^{24}$ cm^{-2} (Buchner et al. 2015). If we estimate the width ΔD of the torus – measured from the inner boundary to the outer one of the torus – we can derive $n_{\rm ext}$ approximately by $N_H/(\Delta D)$. To estimate ΔD, we use two pieces of empirical information: (i) there is a correlation between AGN luminosity and the radius of the inner boundary of the torus (Nenkova et al. 2008), according to which the inner boundary is at 0.2 pc for our typical AGN with a luminosity of $L \simeq 1.6 \times 10^{44}$ erg s^{-1}, and (ii) the outer boundary is typically 10 times more distant than the inner one (Elitzur 2007), so it is at 2 pc in our case. As a result, we find $\Delta D \simeq 1.8$ pc, and hence $n_{\rm ext} \simeq 1.8 \times 10^5$ cm^{-3}.

With the numbers that we have derived for $v_{\rm ext}$ and $n_{\rm ext}$, we proceed to calculate the external pressure with $P_{\rm ext} = m_p n_{\rm ext} v_{\rm ext}^2$, and the result is 2.9×10^{-5} erg cm^{-3}. We find that $P_{\rm ext}$ is consistent with P_S within a factor two. This agreement supports our proposal that the clumps are confined by an external pressure and are dynamically stable.

We note that the radiation from the central AGN cannot be another source of external pressure. This is so, because a dusty cloud exposed to AGN irradiation will evaporate within one orbital period (Pier & Voit 1995; Namekata et al. 2014). The radiative pressure would be

$$P_{\rm rad} = L/(4\pi D^2 c), \tag{23}$$

with c the speed of light. We can see that this value is 5.1×10^{-3} erg cm^{-3}, more than two orders of magnitude higher than the surface pressure P_S derived above for the clump. Hence, for the clump to not be dissolved, it must be shielded during most of its orbital phase by the gas or other clumps located closer to the central SMBH, as has been suggested by Krolik & Begelman (1988); Namekata et al. (2014). Our result, hence, supports this shielding.

3.2. *Clumps in the CND of the Milky Way*

Controversy: Molecular clumps have been detected in the centers of quiescent galaxies as well (Hunt & Malkan 2004; Mazzalay et al. 2013; Davies et al. 2014). In the GC, in particular, tens of molecular clumps reside in the CND, a ring-like (narrow projected width) structure surrounding Sgr A*. The observable parameters and their typical values are $D = 1.8$ pc, $R_c = 0.25$ pc, and $\sigma = 11$ km s^{-1} (from Christopher et al. 2005), and the central SMBH has a well-established mass of $M_\bullet \approx 4 \times 10^6 M_\odot$ (Genzel et al. 2010).

There exists two different methods to derive the masses of these clumps. However, both lead to dilemmas that seem to invalidate the method. We now explain the methods and the problems that emerge with them.

(i) The typical mass of the clump according to the conventional Virial theorem, $M_0 = 3R\sigma^2/(aG)$, is about $3.4 \times 10^4 M_\odot$ (also see Shukla et al. 2004; Christopher et al. 2005; Montero-Castaño et al. 2009; Tsuboi & Miyazaki 2012). A clump with this mass has a density of 2.3×10^7 cm^{-3}, comparable to the tidal density $n_{\rm tide} \simeq 2.8 \times 10^7$ cm^{-3} at the observed distance (D), so the clump can withstand the tidal force. This argument has been used to support the validity of taking M_0 as the real clump mass. However, this mass has two problems. (a) In the context of the conventional Virial theorem, such clumps are gravitationally unstable, as discussed in points 3 and 4 of the list in Section 2.1. They will disappear on a free-fall timescale (about 10^4 yr), shorter than

the required time to form an axisymmetric CND (about 10^5 yr, comparable to the orbital period). In the EVT, however, tidally-locked clumps with this mass are stable, as we will see later. (b) Nonetheless, M_0 is likely to be ruled out, because if this were indeed the real mass of the clumps, then the CND would have a total mass of about 10^6 $M_\odot$. Such a heavy disk would inevitably destroy the *observed* young stellar disk within 0.5 pc around Sgr A* (Šubr et al. 2009).

(ii) Another way of deriving the mass of clumps is based on the assumption of local thermal equilibrium (LTE, and in this case we call the mass derived $M_{\rm LTE}$). Several authors obtained a similar result, typically $M_{\rm LTE} \simeq 2.6 \times 10^3$ $M_\odot$, *one order of magnitude smaller than before* (from Tsuboi & Miyazaki 2012, also see Marr et al. 1993; Marshall et al. 1995; Christopher et al. 2005; Liu et al. 2013; Requena-Torres et al. 2012). In this case, $M_{\rm LTE}$ does not lead to the aforementioned problem related to the existence of the young stellar disk in our GC. However, according to the naive tidal limit criterion, these clumps will disappear within a relatively short time, in any case shorter than the required time to form an axisymmetric CND, as has been noticed by these authors.

Solution: We will see that in the context of the EVT, M_0, as derived in (i), is unstable for non-rotating clumps but stable for tidally-locked ones. Nevertheless this does not change the fact that this mass leads to a scenario ruled out by observations. On the other hand, a clump with mass $M_{\rm LTE}$, as derived in (ii) can be stable. Since this mass does not lead to contradictions with observations of the GC, it is a realistic value for clumps in the CND.

We now derive the value of P_S as provided by the EVT, and then we will compare it with the environmental pressures independently derived in other means, to prove that the clump with a mass of $M_{\rm LTE}$ is in hydrostatic equilibrium.

The GC nuclear cluster has $\gamma = 1.75$, and the enclosed stellar mass is approximately

$$M_*(D) \simeq 1.6 \times 10^6 D_1^{1.25}. \qquad (24)$$

This stellar distribution is adopted from the early work of Vollmer & Duschl (2000); Christopher et al. (2005) for the sake of comparison, but it is not significantly different from the distribution derived from more recent observations (Genzel et al. 2010). With this stellar component, we find $\sigma' = 14$ km s^{-1} for a non-rotating clump and $\sigma' = 19$ km s^{-1} for a tidally-locked one.

For the non-rotating clump, we hence derive $M_0' \simeq 5.9 \times 10^4$ $M_\odot$, $\alpha_-' = M_{\rm LTE}/M_0' \simeq 0.044 \ll 1$, $\beta' \simeq 4\alpha_-' \simeq 0.18$, and finally $P_S \simeq 6.7 \times 10^{-6}$ erg cm^{-3}. For the tidally-locked one, $M_0' = 1.1 \times 10^5$ $M_\odot$, $\alpha_-' \simeq 0.024$, $\beta' \simeq 0.094$, and $P_S \simeq 1.2 \times 10^{-5}$ erg cm^{-3}. In the two cases, we have $\alpha_-' < (1/2)$, so we can conclude that $M = M_{\rm LTE}$ is a stable solution. We also note that $M = M_0$ is an unstable solution for non-rotating clumps, but it could be a stable solution for tidally-locked ones, although, as mentioned before, this mass is excluded because of other arguments not related to the EVT.

Balancing this surface pressure requires an environ-

mental pressure of at least the same order of magnitude. In the GC we have three possibilities: First, the hot, ionized gas in the innermost pc of the GC has a density of 10^4 cm^{-3} (Jackson et al. 1993) and a temperature of 7,000 K (Roberts & Goss 1993), which provides a thermal pressure of $\sim 10^{-8}$ erg cm^{-3}. This pressure is too weak to explain the magnitude of P_S. Any derivation of the mass of the clumps based on this pressure will lead to a too small value, such as the 15 $M_\odot$ derived by (Vollmer & Duschl 2001a). Second, at a distance of $D = 1$ pc, the ram pressure caused by the stellar winds from the observed young stars is about 1.1×10^{-7} erg cm^{-3} (Yusef-Zadeh & Wardle 1993), which is still too weak. The last possibility offers a plausible solution: The molecular gas in the CND, i.e. the "inter-clump" gas, has a turbulent velocity of 55 km s^{-1} (Güsten et al. 1987) and a mean number density of 10^5 cm^{-3} (Genzel et al. 1985). The corresponding pressure due to turbulent motion is 5×10^{-6} erg cm^{-3}, consistent with P_S as derived above. Hence, the clumps in the CND can be stabilized by the inter-clump turbulent gas.

The turbulence of the inter-clump gas has been postulated to be generated by a recent outburst of Sgr A* and continuously replenished by the dissipation of the differential rotation of the CND (Güsten et al. 1987). We have now a number of evidences suggesting that the outburst took place about 6 Myr ago and the bolometric luminosity was as high as 10^{43} erg s^{-1} (e.g. Nayakshin & Cuadra 2005; Su et al. 2010; Bland-Hawthorn et al. 2013; Amaro-Seoane & Chen 2014; Chen & Amaro-Seoane 2014, 2015). This luminosity has a direct, incident radiative pressure on the inner rim of the CND (at about $D = 1$ pc), of about 3×10^{-6} erg cm^{-3} (see Equation 23). This value is comparable to P_S as well as to the turbulent gas pressure. Therefore, we infer that during the outburst of Sgr A*, the inner rim of the CND was pressurized by the radiation and that the pressure propagated into the CND to stabilize the clumps in the context of the EVT.

3.3. *Clumps in the CMZ*

Controversy: The methods (i) and (ii) described in Section 3.2 have been applied to the clumps in the CMZ of the Milky Way to derive their masses. The result is that the virial mass M_0 is on average 10 times larger than $M_{\rm LTE}$ (Miyazaki & Tsuboi 2000; Oka et al. 2001), a difference as large as we have seen in Section 3.2.

Miyazaki & Tsuboi (2000) investigated the possibility that the clumps in the CMZ are confined by the hot, inter-clump ISM. However, the pressure of the hot ISM, obtained from the observations of the 6.7 keV iron lines, is ten times smaller than the surface pressure that one derives based on the conventional Virial theorem (not the EVT). Therefore, the external pressure could not explain the discrepancy.

Partial solution: We adopt now $D = 100$ pc, $R_c = 10$ pc, and $\sigma = 10$ km s^{-1} as the fiducial values (from Oka et al. 2001), but we note that the CMZ spans a large radial range, and the clumps in it have a broad distribution in size as well as in internal velocity dispersion.

In Section 2.3 we addressed two particular cases, namely tidally-locked and non-rotating clumps. In the following, we will show that it is the case of non-rotating clumps what (partially) solves the present problem re-

lated to the clumps in the CMZ.

It does so, because the effective velocity dispersion σ' is smaller than the conventional one σ. Consequently, applying the Virial theorem without accounting for the tidal forces will lead to an overestimation of the surface pressure of the clump. We can see this by comparing the conventional and the extended Virial theorems, i.e. Equations 6 and 16. Physically, this can be envisaged as the result of ignoring the contribution of the compressive tides in the stabilization of the clumps.

According to Equations (20) and given that $2-\gamma > 0$ in the Milky Way (Genzel et al. 2010), the situation $\sigma' < \sigma$ will occur, and it happens when the (effective) stellar mass $(2-\gamma)M_*(D)$ enclosed by the orbit of the clump exceeds the mass $M_\bullet$ of the SMBH. The corresponding region is at $D \gtrsim 6.3$ pc, which encompasses the entire CMZ.

To be more quantitative, we scale Equation (20) using the parameters relevant to the clumps in the CMZ (also from Oka et al. 2001) and we find

$$\sigma'^2 \simeq \sigma^2 - (4.3 \text{ km s}^{-1})^2 \, b \left(\frac{R_c}{10 \text{ pc}}\right)^2 \left(\frac{D}{100 \text{ pc}}\right)^{-1.75}. \tag{25}$$

Given $\sigma \sim 10$ km s^{-1} and $D \sim 10^2$ pc, the last equation suggests that if a clump is bigger than 10 pc, its surface pressure will be significantly weaker than what was derived in the early work based on the conventional Virial theorem.

In a survey of the CMZ (Oka et al. 2001), 67 out of 165 molecular clouds have been observed to have a size larger than 10 pc. Limited to these observations, our EVT *partially* resolves the controversy. Other explanation must be sought to fully address the problem (see Section 4 for discussion).

4. DISCUSSIONS AND CONCLUSION

In this paper we analyze the stability of the gas clouds in the central $1-10^2$ pc of a galaxy, in the region around the SMBH and the nuclear star cluster. We have shown that the external forces – external pressure (Section 2.1) and tidal forces (Section 2.2) – play a crucial role in confining and stabilizing the clouds. Based on this understanding, we formulated an *extended Virial theorem* (or EVT) to identify the correct ranges of physical quantities that lead to stability (Section 2.3). We applied our EVT to model observational data and have solved practical problems related to the stability of those gas clumps detected in AGN tori (Section 3.1), the CND in the GC (Section 3.2), and the CMZ of the Milky Way (Section 3.3, in this last case we partially resolved the problem).

4.1. *Validity of the Assumption of Static Equilibrium*

In the previous sections we have relied on the assumption that the clouds are in hydrostatic equilibrium. However, there are two kinds of perturbations that potentially could invalidate this assumption. (i) Collisions with other clouds could drive a test cloud out of equilibrium, if the cloud number density is high enough. We define $t_{\rm coll}$ as the collisional timescale – the mean timespan during consecutive collisions. (ii) The effect of in-

homogeneity in the ISM can either compress or decompress a test cloud. The fastest relative velocity between the cloud and the ISM is the Keplerian velocity, therefore the shortest timescale for the cloud to return to the inhomogeneous region is the orbital period, $t_{\rm orb}$.

After one perturbation, the cloud requires at least the sound crossing timescale $t_{\rm sc} \simeq 2R_c/\sigma$ to relax and restore equilibrium. So our assumption of hydrostatic equilibrium is valid if these two criteria are simultaneously met: (i) $t_{\rm sc} < t_{\rm coll}$ and (ii) $t_{\rm sc} < t_{\rm orb}$. We now use these two criteria to assess the destabilizing effects in the three different media that we have considered in this paper.

(a) For a cloud in AGN torus, since we know the typical values for σ, R_c, D, $M_\bullet$, we find that $t_{\rm sc} \simeq 42$ yr, $t_{\rm orb} \simeq 6.3\times10^2$ yr. Since Krolik & Begelman (1988) proved that $t_{\rm coll} \simeq t_{\rm orb}$, we conclude that hydrostatic equilibrium can be achieved in AGN tori.

(b) For a cloud in the CND, we find $t_{\rm sc} \simeq 4.5 \times 10^4$ yr and $t_{\rm orb} \simeq 1.1 \times 10^5$ yr using the observational data. From the numerical simulations of Vollmer & Duschl (2002), we have that $t_{\rm coll} \simeq 2$ Myr. Hence, hydrostatic equilibrium can be achieved in the CND.

(c) For a cloud in the CMZ, we derive $t_{\rm sc} \simeq 2$ Myr and $t_{\rm orb} \simeq 5.9$ Myr according to the observational data. For $t_{\rm coll}$, we notice that the clumps cover about 50% of the disk area (Oka et al. 2001), so we use the formula for $t_{\rm coll}$ derived in Bally et al. (1988), which is a function of the covering factor, and we find $t_{\rm coll} \simeq 4$ Myr for a cloud at $D = 100$ pc. In this region, the three timescales (i.e. $t_{\rm sc}$, $t_{\rm coll}$, and $t_{\rm orb}$) are of the same order of magnitude. As a result, the clouds may not have had enough time to fully restore equilibrium. This could be the reason why in Section 3.3 we only could explain a fraction of the clumps in the CMZ. Indeed, there is evidence that at the inner rim of the CMZ, where both $t_{\rm coll}$ and $t_{\rm orb}$ are relatively short, the molecular clouds may have recently experienced collisions (e.g. Rodriguez-Fernandez et al. 2006).

4.2. *Conclusion*

We have proven that the observed gas clumps in AGNs tori and in the CND of the Milky Way (and partially in the CMZ) are not self-gravitating, but instead, they are stabilized by external pressure and tidal forces. The standard Jeans instability produces only self-gravitating clouds, and therefore it cannot account for the origin of these observed clumps.

The noticeably large internal energy relative to the self-gravity, as we found for these clumps, is more consistent with a non-conventional formation mechanism, such as the collisional fragmentation and agglomeration (Krolik & Begelman 1988; Vollmer et al. 2004). This discovery supports the picture that clump-clump collision drives gas inflow to the central pc to power AGNs .

In the future, application of the EVT to individual clumps (i.e. observed clouds) potentially can provide us with a mapping of clump masses and environmental pressure around supermassive black holes in galactic nuclei.

REFERENCES

Amaro-Seoane, P. 2012, ArXiv e-prints
Amaro-Seoane, P. & Chen, X. 2014, ApJ, 781, L18
Antonucci, R. 1993, ARA&A, 31, 473
Bally, J., Stark, A. A., Wilson, R. W., & Henkel, C. 1988, ApJ, 324, 223
Bland-Hawthorn, J., Maloney, P. R., Sutherland, R. S., & Madsen, G. J. 2013, ApJ, 778, 58
Buchner, J., Georgakakis, A., Nandra, K., Brightman, M., Menzel, M.-L., Liu, Z., Hsu, L.-T., Salvato, M., Rangel, C., Aird, J., Merloni, A., & Ross, N. 2015, ApJ, 802, 89
Burkert, A. & Lin, D. N. C. 2000, ApJ, 537, 270
Chen, X. & Amaro-Seoane, P. 2014, ApJ, 786, L14
—. 2015, Classical and Quantum Gravity, 32, 064001
Christopher, M. H., Scoville, N. Z., Stolovy, S. R., & Yun, M. S. 2005, ApJ, 622, 346
Clausius, R. 1870, Annalen der Physik, 217, 124
Collin, S. & Zahn, J.-P. 2008, A&A, 477, 419
Davies, R. I., Maciejewski, W., Hicks, E. K. S., Emsellem, E., Erwin, P., Burtscher, L., Dumas, G., Lin, M., Malkan, M. A., Müller-Sánchez, F., Orban de Xivry, G., Rosario, D. J., Schnorr-Müller, A., & Tran, A. 2014, ApJ, 792, 101
Elitzur, M. in , Astronomical Society of the Pacific Conference Series, Vol. 373, The Central Engine of Active Galactic Nuclei, ed. L. C. HoJ.-W. Wang, 415
Elvis, M. 2000, ApJ, 545, 63
Fabian, A. C. 2012, ARA&A, 50, 455
Genzel, R., Crawford, M. K., Townes, C. H., & Watson, D. M. 1985, ApJ, 297, 766
Genzel, R., Eisenhauer, F., & Gillessen, S. 2010, Reviews of Modern Physics, 82, 3121
Gladman, B., Quinn, D. D., Nicholson, P., & Rand, R. 1996, Icarus, 122, 166
Goodman, J. 2003, MNRAS, 339, 937
Goodman, J. & Tan, J. C. 2004, ApJ, 608, 108
Güsten, R., Genzel, R., Wright, M. C. H., Jaffe, D. T., Stutzki, J., & Harris, A. I. 1987, ApJ, 318, 124
Hunt, L. K. & Malkan, M. A. 2004, ApJ, 616, 707
Jackson, J. M., Geis, N., Genzel, R., Harris, A. I., Madden, S., Poglitsch, A., Stacey, G. J., & Townes, C. H. 1993, ApJ, 402, 173
Kormendy, J. & Ho, L. C. 2013, ARA&A, 51, 511
Krolik, J. H. & Begelman, M. C. 1988, ApJ, 329, 702
Krolik, J. H. & Lepp, S. 1989, ApJ, 347, 179
Kumar, P. 1999, ApJ, 519, 599
Liu, H. B., Ho, P. T. P., Wright, M. C. H., Su, Y.-N., Hsieh, P.-Y., Sun, A.-L., Kim, S. S., & Minh, Y. C. 2013, ApJ, 770, 44
Maciejewski, W., Teuben, P. J., Sparke, L. S., & Stone, J. M. 2002, MNRAS, 329, 502
Markowitz, A. G., Krumpe, M., & Nikutta, R. 2014, MNRAS, 439, 1403
Marr, J. M., Wright, M. C. H., & Backer, D. C. 1993, ApJ, 411, 667

Marshall, J., Lasenby, A. N., & Harris, A. I. 1995, MNRAS, 277, 594
Mazzalay, X., Saglia, R. P., Erwin, P., Fabricius, M. H., Rusli, S. P., Thomas, J., Bender, R., Opitsch, M., Nowak, N., & Williams, M. J. 2013, MNRAS, 428, 2389
McNamara, B. R. & Nulsen, P. E. J. 2007, ARA&A, 45, 117
Merritt, D. 2010, ApJ, 718, 739
Mezger, P. G., Duschl, W. J., & Zylka, R. 1996, A&A Rev., 7, 289
Miyazaki, A. & Tsuboi, M. 2000, ApJ, 536, 357
Montero-Castaño, M., Herrnstein, R. M., & Ho, P. T. P. 2009, ApJ, 695, 1477
Namekata, D., Umemura, M., & Hasegawa, K. 2014, MNRAS, 443, 2018
Nayakshin, S. & Cuadra, J. 2005, A&A, 437, 437
Nenkova, M., Sirocky, M. M., Nikutta, R., Ivezić, Ž., & Elitzur, M. 2008, ApJ, 685, 160
Netzer, H. 2015, ArXiv e-prints
Oka, T., Hasegawa, T., Sato, F., Tsuboi, M., Miyazaki, A., & Sugimoto, M. 2001, ApJ, 562, 348
Pier, E. A. & Voit, G. M. 1995, ApJ, 450, 628
Rees, M. J. 1987, MNRAS, 228, 47P
Requena-Torres, M. A., Güsten, R., Weiß, A., Harris, A. I., Martín-Pintado, J., Stutzki, J., Klein, B., Heyminck, S., & Risacher, C. 2012, A&A, 542, L21
Risaliti, G., Elvis, M., & Nicastro, F. 2002, ApJ, 571, 234
Roberts, D. A. & Goss, W. M. 1993, ApJS, 86, 133
Rodriguez-Fernandez, N. J., Combes, F., Martin-Pintado, J., Wilson, T. L., & Apponi, A. 2006, A&A, 455, 963
Shlosman, I., Begelman, M. C., & Frank, J. 1990, Nature, 345, 679
Shu, F. H. 1992, The physics of astrophysics. Volume II: Gas dynamics.
Shukla, H., Yun, M. S., & Scoville, N. Z. 2004, ApJ, 616, 231
Shull, J. M. 1978, ApJ, 226, 858
Spitzer, L. 1978, Physical processes in the interstellar medium
Stark, A. A. & Blitz, L. 1978, ApJ, 225, L15
Su, M., Slatyer, T. R., & Finkbeiner, D. P. 2010, ApJ, 724, 1044
Tan, J. C. & Blackman, E. G. 2005, MNRAS, 362, 983
Tsuboi, M. & Miyazaki, A. 2012, PASJ, 64, 111
Šubr, L. ., Schovancová, J., & Kroupa, P. 2009, A&A, 496, 695
Vollmer, B., Beckert, T., & Duschl, W. J. 2004, A&A, 413, 949
Vollmer, B. & Duschl, W. J. 2000, New Astron. , 4, 581
—. 2001a, A&A, 367, 72
—. 2001b, A&A, 377, 1016
—. 2002, A&A, 388, 128
Yusef-Zadeh, F. & Wardle, M. 1993, ApJ, 405, 584
Zwicky, F. 1937, ApJ, 86, 217